

Article

Not peer-reviewed version

---

# Effect of Film Thickness on Microstructural and Magnetic Properties of Lithium Ferrite Films Prepared on $\text{SrTiO}_3$ (001) Substrates

---

[Kun Liu](#) , Ruyi Zhang , [Lu Lu](#) \* , Jiankang Li , Songyou Zhang

Posted Date: 25 September 2023

doi: 10.20944/preprints202309.1631.v1

Keywords: Lithium ferrite; film thickness; defects; magnetic properties; electron microscopy



Preprints.org is a free multidiscipline platform providing preprint service that is dedicated to making early versions of research outputs permanently available and citable. Preprints posted at Preprints.org appear in Web of Science, Crossref, Google Scholar, Scilit, Europe PMC.

Copyright: This is an open access article distributed under the Creative Commons Attribution License which permits unrestricted use, distribution, and reproduction in any medium, provided the original work is properly cited.

Disclaimer/Publisher's Note: The statements, opinions, and data contained in all publications are solely those of the individual author(s) and contributor(s) and not of MDPI and/or the editor(s). MDPI and/or the editor(s) disclaim responsibility for any injury to people or property resulting from any ideas, methods, instructions, or products referred to in the content.

## Article

# Effect of Film Thickness on Microstructural and Magnetic Properties of Lithium Ferrite Films Prepared on $\text{SrTiO}_3$ (001) Substrates

Kun Liu <sup>1</sup>, Ruyi Zhang <sup>2</sup>, Lu Lu <sup>3,\*</sup>, Jiankang Li <sup>1</sup> and Songyou Zhang <sup>1</sup>

<sup>1</sup> School of Electronics and Information Engineering, Suzhou Vocational University, Su Zhou 215104, China

<sup>2</sup> Ningbo Institute of Materials Technology and Engineering, Chinese Academy of Sciences, Ningbo 315201, China

<sup>3</sup> Ji Hua Laboratory, Foshan 528200, China

\* Correspondence: lulu@jihualab.ac.cn

**Abstract:** Epitaxial lithium ferrite ( $\text{LiFe}_5\text{O}_8$ ) films with different thicknesses have been successfully fabricated on  $\text{SrTiO}_3$  (001) substrates by magnetron sputtering deposition technique. The microstructural and magnetic properties are characterized by advanced transmission electron microscope and magnetic measurement device. It was found that the formation of structural defects can be influenced by the thickness of the film. Apart from the misfit dislocations, the orientation domains form in thinner film and twin boundaries appear in thicker film, respectively, contributing to the misfit strain relaxation in the heterosystem. The magnetic measurement shows that the thinner films have enhanced magnetization and a relatively lower coercive field compared with the thicker films containing the antiferromagnetic twin boundaries. Our results provide a way for tuning the microstructure and magnetic properties of lithium ferrite films by changing the film thickness.

**Keywords:** Lithium ferrite; film thickness; defects; magnetic properties; electron microscopy

## 1. Introduction

Lithium ferrite ( $\text{LiFe}_5\text{O}_8$ ) has drawn widespread attention of research because of its remarkable physical properties, such as high saturation magnetization, high Curie temperature, large electric resistivity, low loss at high frequencies, and good chemical and thermal stability [1,2], which make it have potential application in components of microwave device and spintronics [3,4].  $\text{LiFe}_5\text{O}_8$  has the inverse spinel structure, where the tetrahedral sites are occupied by  $\text{Fe}^{3+}$ , and the octahedral sites are shared by  $\text{Li}^+$  and the rest  $\text{Fe}^{3+}$  in a ratio of 1:3 (denoted as  $\text{Fe}[\text{Li}_{0.5}\text{Fe}_{1.5}]\text{O}_4$ ). The antiparallel aligned magnetic spin between the  $\text{Fe}^{3+}$  distributing at tetrahedral sites and octahedral sites leads to a high magnetic moment of  $2.5 \mu\text{B}$  per formula unit [1,5]. Compared to the bulk material, spinel thin films exhibit microstructural variations such as the presence of planar defects, which can alter the electrical and magnetic structures of the films [6,7]. Thus, research efforts concentrating on the growth, structure, property, and applications of the spinel thin films have proliferated over the last decades [8–10].

Generally, during the film deposition process, many degrees of freedom can be used to modify the structural and physical properties of the film [11–13]. Among them, changing the film thickness is a common method to manipulate the strain state of the film [14,15]. Particularly, tuning strain states not only cause the formation of oriented domains [16,17], but also lead to the different density of antiphase boundaries in spinel films [18,19], which influence the magnetic properties of the films consequently [20]. Moreover, enhanced magnetic moments are present in ultrathin films (e.g.,  $\text{NiFe}_2\text{O}_4$  and  $\text{CoFe}_2\text{O}_4$ ) prepared on spinel-type  $\text{MgAl}_2\text{O}_4$  substrates [21–23]. In contrast, there are limited investigations on the microstructural characteristic and magnetic behavior of  $\text{LiFe}_5\text{O}_8$  films with different thickness prepared on perovskite-type substrates that are widely used as substrates for growing functional films in device application.

In the present work, the microstructural and magnetic properties of  $\text{LiFe}_5\text{O}_8$  films with two different thicknesses prepared on  $\text{SrTiO}_3$  substrates have been investigated by aberration-corrected (scanning) transmission electron microscopy ((S)TEM) and superconducting quantum interference device (SQUID). The twin boundaries (TBs), orientation domains, and interface dislocation in the films have been determined by high-angle annular dark-field (HAADF) imaging. The magnetic properties of the films have been characterized by magnetization measurement in a SQUID magnetometer, and the effect of film thickness and structure defects on the magnetic properties of the  $\text{LiFe}_5\text{O}_8$  films has been discussed.

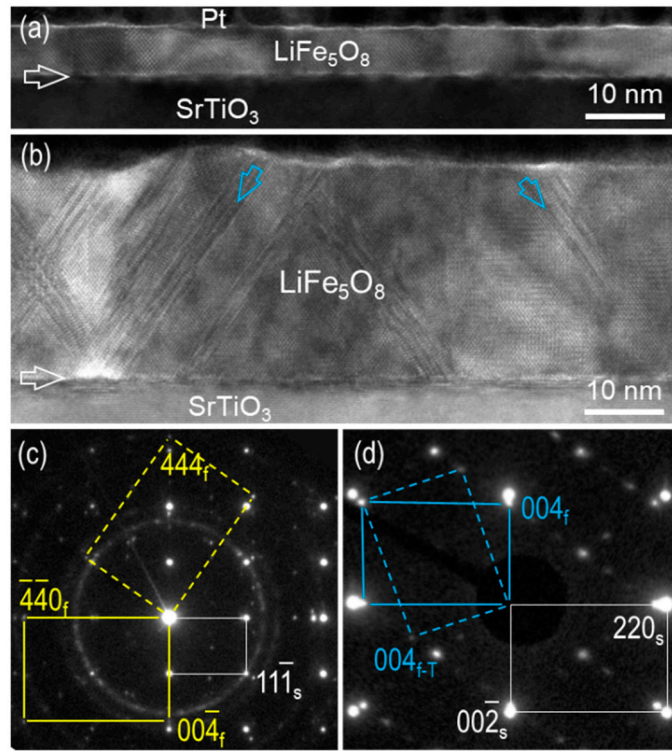
## 2. Materials and Methods

$\text{LiFe}_5\text{O}_8$  ceramic target was prepared by a standard solid-state reaction method with the initial reactants  $\text{Fe}_2\text{O}_3$  and  $\text{LiCO}_3$  (ratio 5:2). The  $\text{LiFe}_5\text{O}_8$  films with different thicknesses were fabricated on single-crystalline  $\text{SrTiO}_3$  (001) substrates by a high-pressure sputtering system at the substrate temperature of 800 °C. The working pressure was 0.5 mbar with the mixed ambient of Ar and  $\text{O}_2$  at the ratio of 1:1.

(S)TEM specimens were prepared by focused ion beam (FIB) lift-out technique using an FEI Helios600i FIB/SEM system. FIB lamellae were cut along the <110> orientations of the  $\text{SrTiO}_3$  substrate. TEM and HAADF-STEM experiments were performed on a JEOL-ARM200F with a probe aberration corrector, operated at 200 kV. In STEM mode, a probe size of 0.1 nm at semi-convergence angle of 22 mrad was used for HAADF-STEM imaging. The HAADF detectors covered angular ranges of 90-176 mrad.

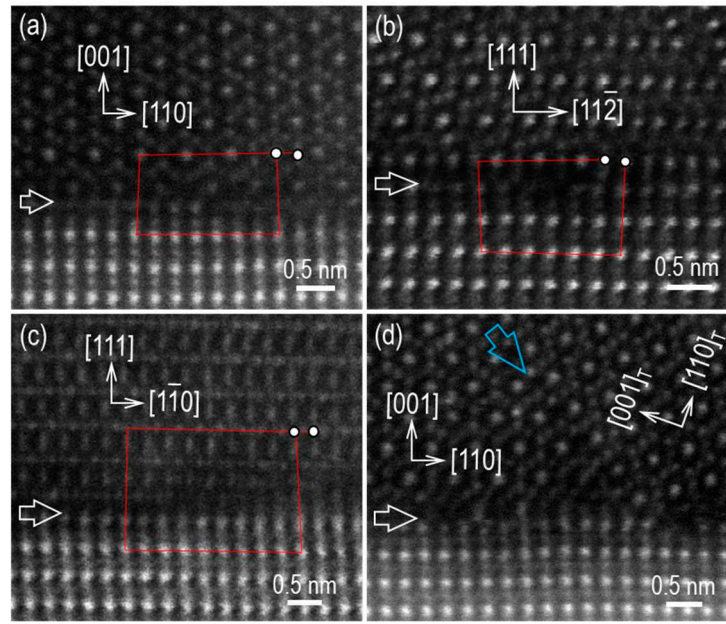
## 3. Results and discussions

Figure 1a and 1b are the low-magnification bright-field (BF) TEM images of  $\text{LiFe}_5\text{O}_8$  thin film on  $\text{SrTiO}_3$ (001) substrates with a thickness of 7.5 nm and 30 nm, respectively. The film-substrate interfaces are marked by horizontal arrows. The contrast variation within the film can be discerned in both films. In Figure 1b, the oblique contrast lines shown by blue arrows are apparent. Figure 1c and 1d display the corresponding selected area electron diffraction (SAED) pattern of the heterostructure in Figure 1a and 1b, respectively, recorded along the [1̄10] zone axis of  $\text{SrTiO}_3$ . In Figure 1c, apart from the diffraction spots of the  $\text{SrTiO}_3$  substrate, two sets of diffraction spots from the  $\text{LiFe}_5\text{O}_8$  film can be distinguished, resulting in two film-substrate orientation relationships (ORs) as [110](001)<sub>film</sub>//[1̄10](001)<sub>substrate</sub> (cube-on-cube) and [110](111)<sub>film</sub>//[1̄10](001)<sub>substrate</sub>. Considering the four-fold symmetry of the  $\text{SrTiO}_3$ (001) substrate surface, there exists an equivalent OR having a 90° in-plane orientation relation to the latter OR. In Figure 1d, the  $\text{LiFe}_5\text{O}_8$  film adopts the cube-on-cube OR with the substrate. Instead of forming crystalline orientation domains in the 7.5-nm-thick film, there present some {111} TBs in the 30-nm-thick film. Taking the lattice parameter of  $\text{SrTiO}_3$  substrate (0.3905 nm) as the calibration standard [24], the in-plane and out-of-plane lattice parameter of the 7.5-nm-thick film is calculated to be 0.8319 nm and 0.8353 nm, respectively. Similarly, in-plane and out-of-plane lattice parameter of the 30-nm-thick film is calculated to be 0.8301 nm and 0.8359 nm, respectively. Both films are under the compressive strain along the in-plane direction [10].



**Figure 1.** (a, b) Low-magnification BF-TEM images and (c, d) the corresponding SAED patterns of 7.5-nm-thick and 30-nm-thick LiFe<sub>5</sub>O<sub>8</sub> film prepared on SrTiO<sub>3</sub> (001) substrate, recorded along the [1-10] SrTiO<sub>3</sub> zone axes. The film-substrate interface is indicated by horizontal arrows. The twin boundary is denoted by oblique blue arrows.

In order to further investigate the microstructure and strain relaxation behaviors, high-resolution HAADF-STEM experiments have been performed. Figure 2a-c are the atomic-resolution HAADF-STEM images showing the interfaces of the 7.5-nm-thick film, viewed along [1-10] zone axis of the SrTiO<sub>3</sub> substrate. Misfit dislocations form at the interface in both heterostructures. For the grain with the cube-on-cube OR (Figure 2a), the projected Burgers vector of misfit dislocations can be determined as  $(a_f/4)[110]$  ( $a_f$  is the lattice parameter of LiFe<sub>5</sub>O<sub>8</sub>). For the [1-10](111)<sub>film</sub>//[1-10](001)<sub>substrate</sub> OR, the misfit dislocations occur at the interfaces, as shown in Figure 2b,c. The projected Burgers vectors are determined to be  $(a_f/8)[1\bar{1}\bar{2}]$  and  $(a_f/4)[1\bar{1}0]$ , respectively. In contrast, for the heterostructure of the 30-nm-thick film on the SrTiO<sub>3</sub>(001) substrate, only a number of {111} TBs appear within the LiFe<sub>5</sub>O<sub>8</sub> film as demonstrated in Figure 2d.



**Figure 2.** (a-d) High-resolution HAADF-STEM images of the heterostructures, viewed along the  $[1\bar{1}0]$   $\text{SrTiO}_3$  zone axis, showing the formation of misfit dislocations and twin boundaries. The film-substrate interfaces are denoted by horizontal white arrows.

Additionally, for the heterostructure of the 7.5-nm-thick film prepared on  $\text{SrTiO}_3(001)$  substrate, the occurrence of two types of film-substrate ORs would form a columnar grain structure in the film. The coalescence of these grains inevitably leads to the formation of grain boundaries (GBs). Figure 3a-c are the HAADF-STEM images containing such GBs. The boundaries appear curved through the film as traced by white dashed lines. It should be emphasized that there is no secondary phase or obvious element segregation at the boundaries.

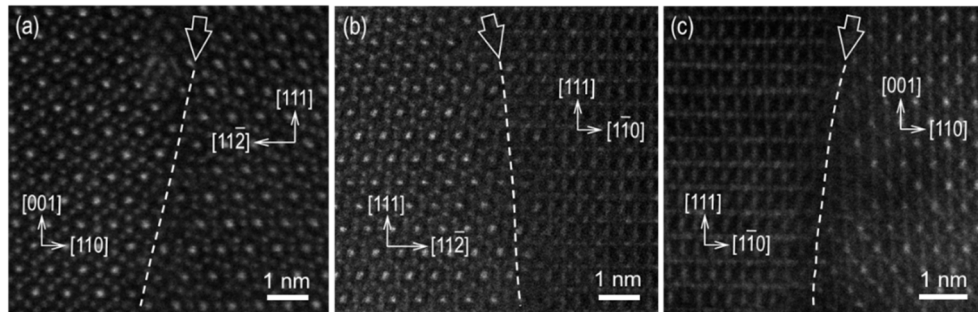


**Figure 3.** (a-c) HAADF-STEM images of grain boundaries in 7.5-nm-thick film. The boundaries are denoted by white dashed lines and oblique white arrows.

In the  $\text{LiFe}_5\text{O}_8/\text{SrTiO}_3$  heterostructure, the lattice mismatch is calculated to be about +6.2% for cube-on-cube epitaxy, using the formula  $[(a_f - 2a_s)/2a_s] * 100\%$ . For the  $\text{LiFe}_5\text{O}_8(111)/\text{SrTiO}_3(001)$  epitaxy, the lattice mismatch along  $[110]_f$  direction is the same as that of the cube-on-cube epitaxy, whereas the film-substrate lattice mismatch along  $[11\bar{2}]_f$  direction is much large. According to our experimental results, the strain relaxation behaviors are essentially different for the  $\text{LiFe}_5\text{O}_8$  films with different thicknesses prepared on  $\text{SrTiO}_3(001)$  substrates. The appearance of oriented grains and misfit dislocations releases the compressive strain in the 7.5-nm-thick film on  $\text{SrTiO}_3$  substrate. In contrast, the formation of a high density of twins within the film mainly contributes to the strain relaxation in the 30-nm-thick film.

The magnetic properties of the  $\text{LiFe}_5\text{O}_8$  films have been characterized by the magnetic hysteresis loops using the SQUID system. The effect of pure  $\text{SrTiO}_3$  substrate has been carefully eliminated.

Figure 4a,b present the M-H hysteresis loops measured along in-plane and out-of-plane directions of 7.5-nm- and 30-nm-thick film separately. The in-plane saturation magnetization ( $M_s$ ) of the 7.5-nm-thick film is about 535 emu/cc and the out-of-plane  $M_s$  is 443 emu/cc. Both values are significantly higher than that of bulk  $\text{LiFe}_5\text{O}_8$  (2.5  $\mu\text{B}/\text{formula unit}$   $\sim$  320 emu/cc) [5]. The in-plane and the out-of-plane  $M_s$  of the 30-nm-thick film are about 194 emu/cc and 137 emu/cc, respectively. The in-plane and out-of-plane coercive fields ( $H_c$ ) of the 7.5-nm-thick film are about 71 Oe and 142 Oe, respectively, which are smaller than that of the 30-nm-thick film (217 Oe and 166 Oe). Our measurement of the magnetic properties shows apparent thickness dependence of  $\text{LiFe}_5\text{O}_8$  thin films prepared on  $\text{SrTiO}_3(001)$  substrates.

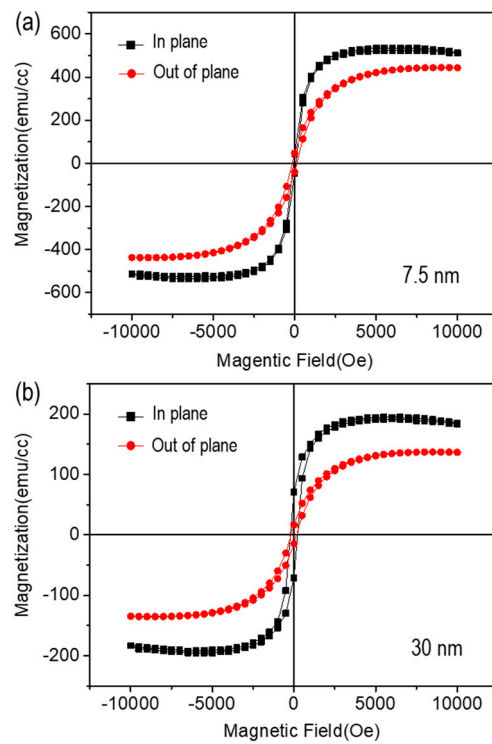


**Figure 4.** (a, b) In-plane and out-of-plane magnetic hysteresis loops of  $\text{LiFe}_5\text{O}_8$  films with different thicknesses measured at room temperature (300 K).

The enhancement of the magnetic moment and the decrease of the coercive field has been reported in thinner spinel films, e.g.,  $\text{NiFe}_2\text{O}_4$  and  $\text{CoFe}_2\text{O}_4$  [21–23] and  $\text{LiFe}_5\text{O}_8$  on  $\text{MgAl}_2\text{O}_4$  substrates [10]. The anomalous cation distribution among the tetrahedral and octahedral sites of the spinel structure has been invoked to account for this phenomenon [14,21]. In our  $\text{LiFe}_5\text{O}_8$  thin films, no chemical modulation or second phase has been observed during TEM investigations, ruling out the anomalous  $\text{Fe}^{3+}$  distribution as the origin of the enhanced  $M_s$ . Thus, the most likely factor responsible for the thickness-dependent magnetic properties is the strain state and the microstructure of the film. For the inverse spinel structure materials, the compressive strain favors the in-plane orientation of the magnetization [22,25]. Moreover, the magnetic coupling across the nonstoichiometric twin boundaries (TBs) in spinel is antiferromagnetic [7]. Although strain relaxations occur in our  $\text{LiFe}_5\text{O}_8$  films, the tetragonal lattice distortions appear in both films under compressive strain, resulting in anisotropic magnetization in the both films. Additionally, the appearance of a high density of antiferromagnetic TBs [26] in the 30-nm-thick film can lower the  $M_s$  of the film. In contrast, the oriented GBs are dominant in the 7.5-nm-thick film, which may enhance the  $M_s$  of the film owing to the magnetic coupling at the interfaces [9,17]. Overall, varying thicknesses of the  $\text{LiFe}_5\text{O}_8$  films on  $\text{SrTiO}_3(001)$  substrate can effectively modify the microstructural and magnetic properties of the film.

#### 4. Conclusion

The epitaxial  $\text{LiFe}_5\text{O}_8$  thin films with the thickness of 7.5 nm and 30 nm have been grown on  $\text{SrTiO}_3$  (001) substrate. Microstructural investigations show that the  $(111)_{\text{film}}//(001)_{\text{substrate}}$  and  $(001)_{\text{film}}//(001)_{\text{substrate}}$  ORs appear in the 7.5-nm-thick film, and TBs occur in the 30-nm-thick film, respectively, which contributes to the lattice misfit strain. Importantly, the 7.5-nm-thick film displays a larger saturation magnetization and a relatively lower coercive field in comparison with the 30-nm-thick film. Our results demonstrate that changing the film thickness could effectively tune the microstructure and magnetic properties in epitaxial LFO thin film.

**Author Contributions:** Conceptualisation, K.L.; investigation, K.L, R.Z; writing—original draft preparation, K.L.; writing—review and editing, L.L., J.L, S.Z.; supervision, L.L. All authors have read and agreed to the published version of the manuscript.

**Funding:** This research was funded by the Guangdong Major Project of Basic and Applied Basic Research (No. 2021B0301030003), the Science and Technology Planning Project of Suzhou City (No. SZS2022015), the Natural Science Foundation of the Jiangsu Higher Education Institutions of China (Grant: 21KJB510022) and Cultivation project of Suzhou vocational University (SVU2021py02).

**Institutional Review Board Statement:** Not applicable.

**Informed Consent Statement:** Not applicable.

**Data Availability Statement:** Not applicable.

**Acknowledgments:** Thanks to Suzhou Key Laboratory of Smart Energy Technology, Jihua Laboratory for the support of experiments of characterization.

**Conflicts of Interest:** The authors declare no conflict of interest.

#### References

1. White, G.O.; Patton, C.E. Magnetic Properties of Lithium Ferrite Microwave Materials, *J. Magn. Magn. Mater.* **1978**, 9(4), 299-317.
2. Sugimoto, M. The Past, Present, and Future of Ferrites, *J. Am. Ceram. Soc.* **1999**, 82(2), 269-280.
3. Lüders, U.; Barthélémy, A.; Bibes, M.; Bouzehouane, K.; Fusil, S.; Jacquet, E.; Contour, J.-P.; Bobo, J.-F.; J.-F. Fontcuberta, J.-F.; Fert, A.  $\text{NiFe}_2\text{O}_4$ : A Versatile Spinel Material Brings New Opportunities for Spintronics, *Adv. Mater.* **2006**, 18(13), 1733-1736.
4. Suzuki, Y. Epitaxial Spinel Ferrite Thin Films, *Annual Review of Materials Research* **2001**, 31, 265-289.
5. Boyraz, C.; Mazumdar, D.; Iliev, M.; Marinova, V.; Ma, J.; Srinivasan, G.; Gupta, A. Structural and magnetic properties of lithium ferrite ( $\text{LiFe}_5\text{O}_8$ ) thin films: Influence of substrate on the octahedral site order, *Appl. Phys. Lett.* **2011**, 98(1), 012507.
6. Wei, J. D.; Knittel, I.; Hartmann, U.; Zhou, Y.; Murphy, S.; Shvets, I. V. et al. Influence of the Antiphase Domain Distribution on the Magnetic Structure of Magnetite Thin Films, *Appl. Phys. Lett.* **2006**, 89(12), 122517.
7. Chen, C. L.; Li, H. P.; Seki, T.; Yin, D. Q.; Sanchez-Santolino, G.; Inoue, K et al. Direct Determination of Atomic Structure and Magnetic Coupling of Magnetite Twin Boundaries, *ACS nano*, **2008**, 12(3), 2662-2668.
8. Udhayakumar, S.; Kumar, G. J.; Kumar, E. S.; Navaneethan, M.; Kamala Bharathi, K. Electrical, Electronic and Magnetic Property Correlation Via Oxygen Vacancy Filling and Scaling-law Analysis in  $\text{LiFe}_5\text{O}_8$  Thin Films Prepared by Pulsed Laser Deposition, *J. Mater. Chem. C* **2022**, 10(40), 15051-15060.
9. Liu, X.; Wu, M.; Qu, K.; Gao, P.; Mi, W. Atomic-Scale Mechanism of Grain Boundary Effects on the Magnetic and Transport Properties of  $\text{Fe}_3\text{O}_4$  Bicrystal Films, *ACS Appl. Mater. and Inter.* **2021**, 13(5), 6889-6896.
10. Zhang, R.; Liu, M.; Lu, L.; Mi, S.B.; Wang, H. Strain-tunable magnetic properties of epitaxial lithium ferrite thin film on  $\text{MgAl}_2\text{O}_4$  substrates, *J. Mater. Chem. C* **2015**, 3(21), 5598-5602.
11. Hu, G.; Choi, J. H.; Eom, C. B.; Harris, V. G.; Suzuki, Y. Structural Tuning of the Magnetic Behavior in Spinel-Structure Ferrite Thin Films, *Phys. Rev. B* **2000**, 62(2), R779-R782.
12. Jing, H.M.; Hu, G.L.; Mi, S.B.; Lu, L.; Liu, M.; Cheng, S.D.; Cheng, S.; Jia, C.L. Microstructure and Electrical Conductivity of  $(\text{Y}, \text{Sr})\text{CoO}_{3-\delta}$  Thin Films Tuned by the Film-Growth Temperature, *J. Alloys Compd.* **2017**, 714, 181-185.
13. Foerster, M.; Rebled, J.M.; Estradé, S.; Sánchez, F.; Peiró, F.; Fontcuberta, J. Distinct Magnetism in Ultrathin Epitaxial  $\text{NiFe}_2\text{O}_4$  Films on  $\text{MgAl}_2\text{O}_4$  and  $\text{SrTiO}_3$  Single Crystalline Substrates, *Phys. Rev. B* **2011**, 84(14), 144422.

